



Supplement of

Are atmospheric PBDE levels declining in central Europe? Examination of the seasonal and semi-long-term variations, gas–particle partitioning and implications for long-range atmospheric transport

Céline Degrendele et al.

Correspondence to: Céline Degrendele (degrendele@recetox.muni.cz)

The copyright of individual parts of the supplement might differ from the CC BY 4.0 License.

Table of Contents

List of Tables

Table S1: Additional information about the air sampling performed.....	S2
Table S2: Range of the limit of quantifications (LOQs)	S2
Table S3: Comparison of the change of sampling preparation on the reported PBDE concentrations.	S3
Table S4: Comparison of the relative response factors (RRF) of individual PBDEs on different analytical columns	S3
Table S5: Results of breakthrough experiments.....	S3
Table S6: Summary of the atmospheric concentrations and detections of individual PBDEs found in this study	S4
Table S7: Results of regression analysis between θ_{measured} and $\log K_p$ and the inverse of temperature for individual congeners.....	S5
Table S8: Results of Spearman correlation analysis between θ_{measured} and the precipitation rate for individual PBDEs.....	S5
Table S9: Results of the Spearman correlation analysis between the individual concentrations of PBDEs and different meteorological parameters.	S5
Table S10: Results of Clausius Clapeyron plots listing slopes, constants, coefficient of determination and confidence level for PBDEs.....	S6
Table S11: Results of the harmonic regression applied to the PBDE dataset.	S6
Table S12: Apparent half lives of individual PBDEs observed in this study and elsewhere.	S7

List of Figures

Figure S1: Results of the breakthrough experiments for BDE47, BDE99, BDE183 and BDE209	S8
Figure S2: Average contribution of individual BDEs to Σ_8 PBDEs.....	S8
Figure S3: Average measured particulate fraction (θ_{measured}) found in this study	S8
Figure S4: Comparison of measured and predicted θ	S9
Figure S5: Comparison of measured and predicted θ for all individual PBDEs in summer and winter	S10
Figure S6: Comparison of the predicted and measured $\log K_p$ and θ using the average conditions at the sampling site.....	S11
Figure S7: Schematic of the effect of an over- or under-estimation of K_p by one order of magnitude in terms of θ	S12
Figure S8: Comparison of the measured particulate fractions (θ_{measured}) of two sets of isomers.	S12
Figure S9: Correlation between the gaseous or the particulate concentration of individual PBDEs with the inverse of temperature.	S14
Figure S10: Selected examples of 5 days backward trajectories of samples associated with the lowest PBDE concentrations	S14
Figure S11: Selected examples of 5 days backward trajectories of samples associated with the highest PBDE concentrations	S15
Figure S12: Multi-years trend of some PBDEs	S16

Temperature dependence of PBDEs

The gas-phase behavior of PBDEs can be described by the Clausius-Clapeyron equation:

$$\ln P = (-\Delta H_v/R)(1/T) + \text{constant} \quad (\text{Eq. S1})$$

where P is partial pressure (Pa), T is temperature (K), ΔH_v is enthalpy of vaporization (kJ.mol⁻¹) and R is the gas constant. The temperature dependence of atmospheric PBDE concentrations was expressed as the linear regressions of the natural logarithm of partial pressure versus the inverse of the temperature: $\ln P = m/T + b$, where m and b are constants. (Eq. S2)

Partial pressures of individual compounds were calculated for each sampling event using gas phase concentrations and the ideal gas law.

Table S1: Additional information about the air sampling performed

Year	Sampled volume (min-max)	Number of samples considered	Number of samples excluded	Number of field blanks	Number of laboratory blanks	Time span covered
2011	4512 ; 5863	40	9	3	2	63%
2012	4015 ; 5864	26	1	3	2	42%
2013	3753 ; 5480	23	3	2	3	38%
2014	5236 ; 5597	25	0	3	4	41%

Table S2: Range of the limit of quantifications (LOQs) determined as the maximum between the instrument (iLOQ) and the field blank concentrations plus three times their standard deviations (LOQ_{blanks}). ND indicates cases for which a compound was not detected in the field blanks. To calculate LOQs in pg m⁻³, the average and representative sample volume (V=5264 m³) was used

	iLOQ (min-max)		LOQ _{blanks} (min-max)
	pg/μL	pg/m ³	pg/ μL
BDE 28	5.20E-03 – 110	4.92E-05 – 1.04	ND – 9.68E-02
BDE 47	2.20E-03 – 41.8	2.09E-05 – 0.40	1.66E-01 – 2.59
BDE 100	3.60E-03 – 5.62	3.50E-05 – 0.05	ND – 5.54
BDE 99	5.40E-03 – 24.8	5.07E-05 – 0.24	0.250 – 2.14
BDE 85	5.00E-03 – 6.20	4.75E-05 – 0.06	ND
BDE 154	5.20E-03 – 4.92	4.84E-05 – 0.05	ND – 0.125
BDE 153	5.80E-03 – 7.64	5.57E-05 – 0.07	ND
BDE 183	1.68E-02 – 11.9	1.59E-04 – 0.11	ND – 650
BDE 209	6.20E-2 – 107	5.90E-04 – 1.02	ND – 60.6

Table S3: Comparison of the change of sampling preparation on the reported PBDE concentrations. Sample preparation 1 was used for samples from 2011-2012 while the sampling preparation 2 was used for samples from 2013 (see Section 2.2 for further details). For each sampling preparation method, 500 pg of each congener was spiked on four PUFs.

	Average amount (pg) from sampling preparation 1	RSD from sampling preparation 1	Average amount (pg) from sampling preparation 2	RSD from sampling preparation 2	Relative difference (%)
BDE 28	481	13	495	14	-3
BDE 47	495	9	481	8	3
BDE 100	526	11	485	14	8
BDE 99	521	12	502	8	4
BDE 85	465	18	498	22	-7
BDE 154	475	8	520	11	-9
BDE 153	534	14	479	12	10
BDE 183	487	9	499	12	-2
BDE 209	564	16	512	18	9

Table S4: Comparison of the relative response factors (RRF) of individual PBDEs on different analytical columns

	RRF DB5 column	RRF RTX-1614 column	% deviation
BDE 28	0.948	0.964	1.7
BDE 47	1.005	0.932	-7.8
BDE 100	1.022	1.047	2.4
BDE 99	0.956	0.981	2.5
BDE 85	0.692	0.674	-2.7
BDE 154	0.899	0.926	2.9
BDE 153	0.935	0.999	6.4
BDE 183	0.856	0.828	-3.4
BDE 209	1.367	1.221	-12.0

Table S5: Results of breakthrough experiments. Only samples for which analytes were detected in at least one of the PUF plugs were considered.

Compound	Frequency of detection on upper PUF	Frequency of detection on lower PUF	% of gas-phase compound mass found on the lower PUF				
			Min	Max	Average	Standard deviation	Median
BDE 28	100%	11.5%	0.0	86.0	5.2	18.1	0.0
BDE 47	92.6%	11.5%	0.0	19.6	2.0	5.7	0.0
BDE 100	74.1%	3.8%	0.0	22.5	1.1	5.0	0.0
BDE 99	66.7%	0%			0.0		
BDE 85	22.2%	0%			0.0		
BDE 154	70.4%	19.2%	0.0	30.1	4.3	8.3	0.0
BDE 153	63%	11.5%	0.0	48.0	5.4	14.0	0.0
BDE 183	55.6%	26.9%	0.0	100.0	24.6	36.2	0.0
BDE 209	3.7%	19.2%	10.1	100.0	82.0	40.2	100.0

Table S6: Summary of the atmospheric concentrations (in pg m^{-3}) and detections (in %) of individual PBDEs found in this study

		BDE 28	BDE 47	BDE 100	BDE 99	BDE 85	BDE 154	BDE 153	BDE 183	BDE 209	$\Sigma_8\text{PBDEs}$
Gas phase	Detection	97	98	75	90	32	87	66	87	41	100
	Min	<LOQ	<LOQ	<LOQ	<LOQ	<LOQ	<LOQ	<LOQ	<LOQ	<LOQ	0.005
	Max	3.731	1.218	0.185	0.570	0.016	0.040	0.054	0.481	4.721	5.858
	Average	0.051	0.140	0.022	0.071	0.003	0.007	0.007	0.023	0.490	0.299
	SD	0.360	0.153	0.027	0.078	0.003	0.006	0.009	0.066	1.027	0.579
Particulate phase	Detection	51	82	89	99	25	90	82	96	79	99
	Min	<LOQ	<LOQ	<LOQ	<LOQ	<LOQ	<LOQ	<LOQ	<LOQ	<LOQ	<LOQ
	Max	0.036	0.312	0.111	0.424	0.039	0.152	0.142	0.367	0.685	1.380
	Average	0.004	0.043	0.017	0.071	0.006	0.023	0.028	0.059	0.257	0.232
	SD	0.006	0.054	0.020	0.082	0.008	0.029	0.030	0.069	0.142	0.285
Total	Detection	98	100	100	100	40	100	91	99	89	100
	Min	<LOQ	0.034	0.001	0.025	<LOQ	0.003	<LOQ	<LOQ	<LOQ	0.084
	Max	3.731	1.251	0.205	0.650	0.039	0.152	0.142	0.511	4.721	6.079
	Average	0.053	0.173	0.031	0.134	0.006	0.027	0.030	0.078	0.457	0.524
	SD	0.359	0.151	0.028	0.098	0.006	0.027	0.029	0.087	0.710	0.611

Table S7: Results of regression analysis between θ_{measured} and $\log K_p$ and the inverse of temperature (K^{-1}) for individual congeners. Numbers in bold indicate cases for which regression coefficients (r^2) were statistically significant ($p<0.05$)

		BDE 28	BDE 47	BDE 100	BDE 99	BDE 85	BDE 154	BDE 153	BDE 183	BDE 209
θ_{measured}	r^2	0.31	0.74	0.55	0.84	0.51	0.76	0.61	0.50	0.06
	slope	1128.62	2353.9	3161.41	3415.06	2919.25	3342.31	2927.09	2062.44	926.44
	intercept	-3.9	-8.12	-10.7	-11.63	-9.92	-11.25	-9.72	-6.6	-2.55
$\log K_p$	r^2	0.38	0.79	0.83	0.80	0.78	0.88	0.80	0.48	0.02
	slope	4169.20	6656.07	6715.63	6934.83	6354.32	7596.57	6783.09	4718.46	-516.98
	intercept	-17.08	-25.66	-25.26	-25.92	-23.72	-27.79	-24.75	-17.43	0.74

Table S8: Results of Spearman correlation analysis between θ_{measured} and the precipitation rate for individual PBDEs. Numbers in bold indicate cases for which the correlations were statistically significant ($p<0.05$)

	BDE 28	BDE 47	BDE 100	BDE 99	BDE 85	BDE 154	BDE 153	BDE 183	BDE 209
precipitation rate	-0.46	-0.44	-0.39	-0.42	-0.31	-0.45	-0.39	-0.40	-0.30
RH	0.38	0.59	0.47	0.62	0.47	0.59	0.47	0.43	0.21

Table S9: Results of the Spearman correlation analysis (r) between the individual concentrations of PBDEs and different meteorological parameters. Numbers in bold indicates cases significant at the 99% confidence interval

	BDE 28	BDE 47	BDE 100	BDE 99	BDE 85	BDE 154	BDE 153	BDE 183	BDE 209
Ctot	precipitation	-0.11	-0.04	-0.18	-0.33	-0.07	-0.52	-0.51	-0.50
	wind direction	-0.26	-0.20	-0.34	-0.38	-0.13	-0.49	-0.50	-0.45
	wind speed	-0.42	-0.51	-0.27	-0.32	-0.11	-0.22	-0.17	-0.11
	RH	-0.07	-0.25	0.08	0.04	0.04	0.35	0.42	0.39
Cg	ABL height	-0.24	-0.24	-0.42	-0.44	-0.20	-0.60	-0.62	-0.57
	Precipitation	-0.06	0.17	0.21	0.14	0.33	0.16	0.23	0.04
	wind direction	-0.22	-0.07	-0.01	0.07	0.23	0.08	0.17	0.21
	wind speed	-0.38	-0.42	-0.25	-0.17	-0.24	-0.24	-0.12	0.00
Cp	RH	-0.18	-0.52	-0.52	-0.53	-0.60	-0.51	-0.42	-0.22
	ABL height	-0.14	0.07	0.13	0.25	0.48	0.21	0.25	0.12
	Precipitation	-0.35	-0.50	-0.49	-0.52	-0.24	-0.50	-0.49	-0.58
	wind direction	-0.33	-0.33	-0.27	-0.36	-0.27	-0.42	-0.42	-0.46
	wind speed	0.01	0.04	-0.11	-0.04	0.36	-0.07	-0.05	-0.10
	RH	0.45	0.48	0.52	0.50	0.60	0.47	0.51	0.45
	ABL height	-0.51	-0.54	-0.57	-0.57	-0.48	-0.54	-0.57	-0.59

Table S10: Results of Clausius Clapeyron plots listing slopes (m), constants (b), coefficient of determination (r^2) and confidence level (p) for PBDEs. For congeners listed in bold, regression parameters are statistically significant at the 99% confidence interval

	r^2	p	N	m	b
BDE 28	0.03	0.08	111	-1747	-24.32
BDE 47	0.43	<0.01	112	-5760	-7.91
BDE 100	0.47	<0.01	85	-7186	-5.08
BDE 99	0.48	<0.01	103	-7078	-4.20
BDE 85	0.61	<0.01	37	-7212	-6.89
BDE 154	0.59	<0.01	99	-7584	-4.88
BDE 153	0.58	<0.01	75	-8308	-2.40
BDE 183	0.19	<0.01	99	-4946	-13.56
BDE 209	0.03	0.28	47	-1951	-21.40

Table S11: Results of the harmonic regression applied to the PBDE dataset. Only the regression coefficients which were statistically significant ($p < 0.05$) are shown

	N	r^2	a_0	a_1	a_2	a_3
BDE28	112	0.07	-19.53	0.28		
BDE47	114	0.10			-0.25	
BDE100	114	0.13	22.54		0.23	-6.40E-04
BDE99	114	0.16	18.30		0.17	-4.98E-04
BDE85	46	0.15				
BDE154	114	0.35			0.69	
BDE153	104	0.29			0.62	-3.93E-04
BDE183	113	0.22			0.59	
BDE209	101	0.21	26.68	0.21		-6.76E-04

Table S12: Apparent half lives ($\tau_{1/2}$) of individual PBDEs observed in this study and elsewhere. Compounds in bold represent the cases which were statistically significant at the 95% confidence interval and ns indicates cases which were not statistically significant.

Reference	This study	Schuster et al; 2010	Birgul et al; 2012			Liu et al; 2013				Shunthirasingham et al; 2018		
Location, type of site	Kosetice, CZ, background site CZ	Background sites UK and NO	London	Manches ter	HAZ	Chicago	Cleveland	St. Point	S.B.D. USA	Burnt Island CA	Point Petre	
Years	2011-2014	2000-2008	2002-2010	2003-2010	2000-2010	2005-2011				2005-2013	2005-2014	
	Half-life	Half-life ± SD	Half-lives (min-max)			Half-life ± SD				Half-life		
BDE 28										26	15	
BDE 47		2.4 ± 0.2				4.6 ± 0.4	5.4 ± 0.7	ns	ns	ns	-23	7.2
BDE 100	2.97 (1.87 ; 7.15)	4.0 ± 0.4				11 ± 3	7.6 ± 1.5	ns	ns	-8.1 ± 2.8	-17	5.9
BDE 99	3.81 (2.48 ; 8.18)	3.3 ± 0.3									13	6.6
BDE 85												
BDE 154		3.3 ± 0.1									1.8	0.95
BDE 153	4.83 (2.57 ; 38.94)	1.4 ± 0.3									2.5	-5
BDE 183												
BDE 209	2.81 (1.91 ; 5.29)					-15 ± 7	7.0 ± 2.0	ns	14 ± 7	16 ± 8	5.7	16
ΣPBDEs			3.4 (2.2-6.9)	2.0 (1.3-4.6)	2.2-9.0	11 ± 3	5.6 ± 0.8	6.3 ± 1.1	ns	ns	-20	8.4

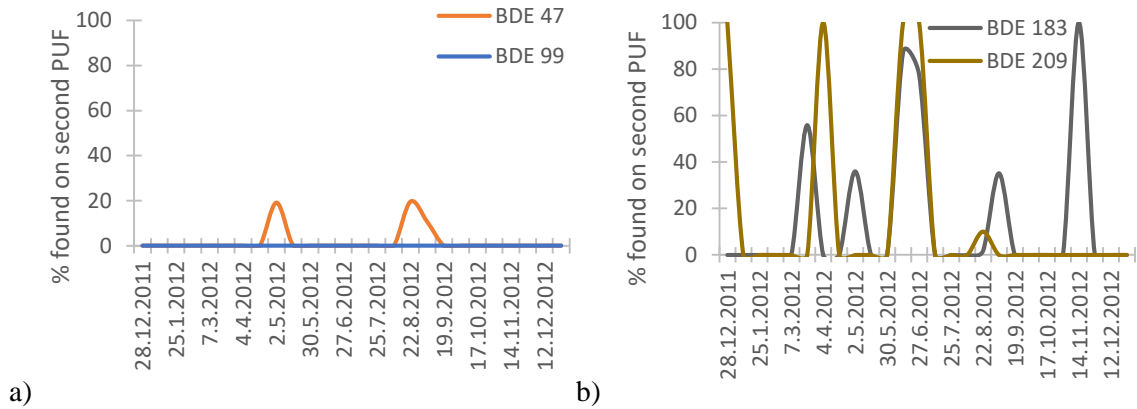


Figure S1: Results of the breakthrough experiments for BDE47, BDE99 (a), BDE183 and BDE209 (b)

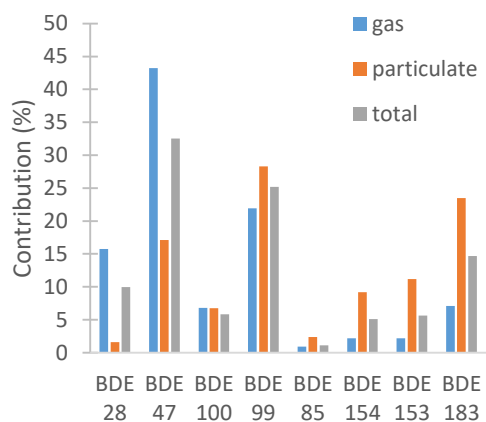


Figure S2: Average contribution of individual BDEs to Σ_8 PBDEs

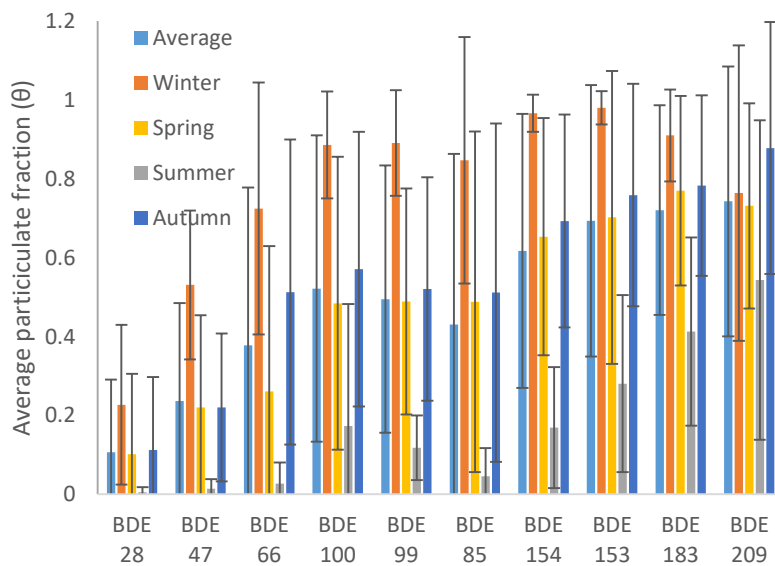


Figure S3: Average measured particulate fraction (θ_{measured}) found in this study

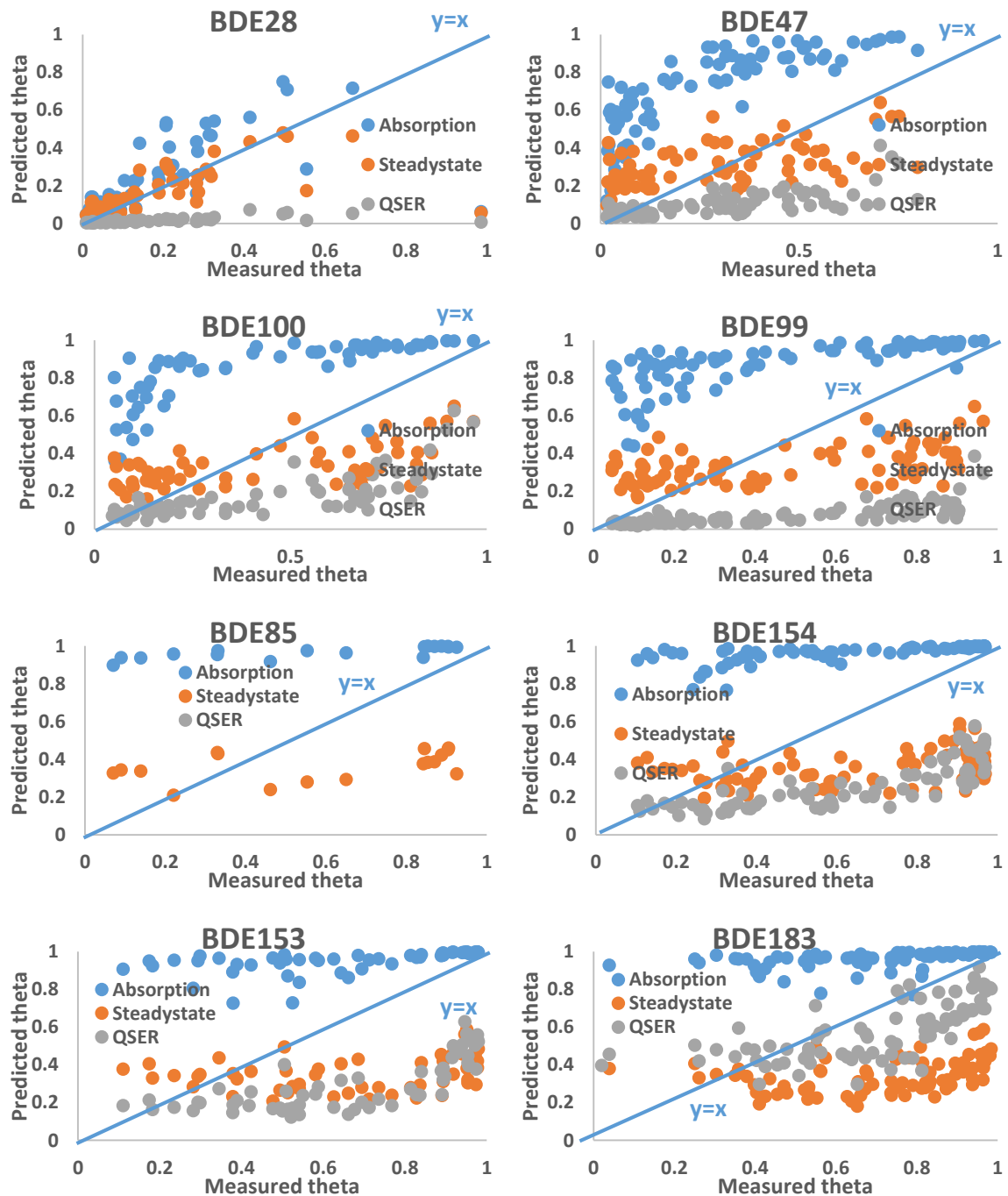
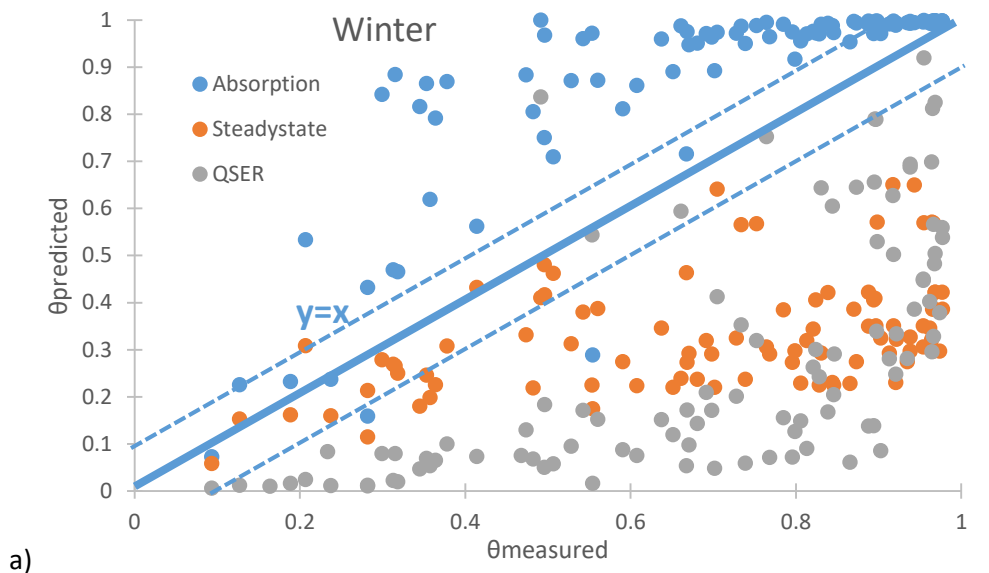
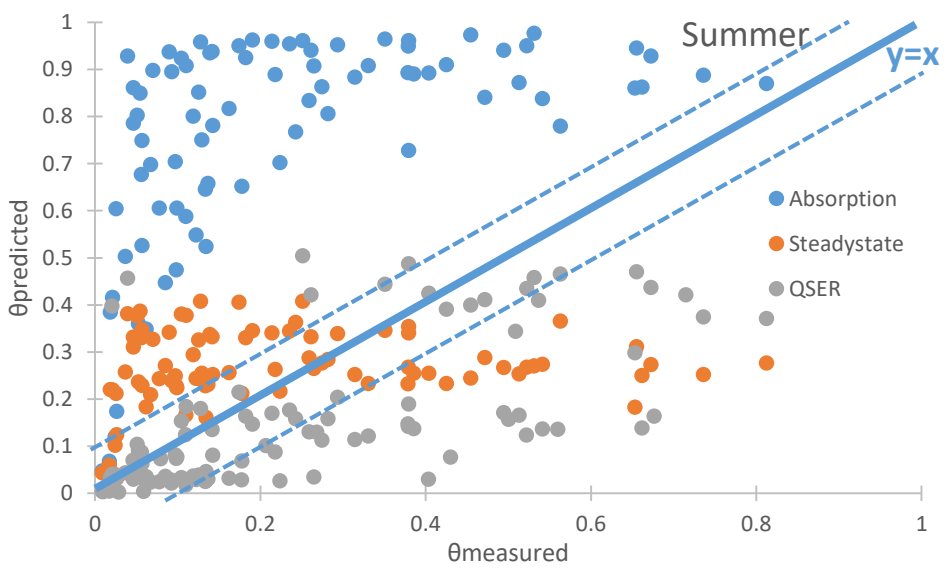


Figure S4: Comparison of measured and predicted θ . No data from the QSPR model were available for BDE85

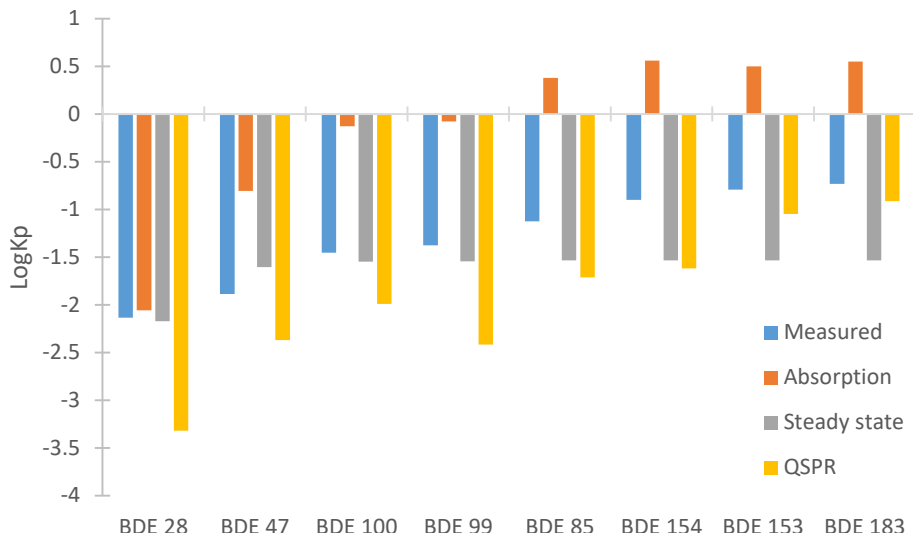


a)

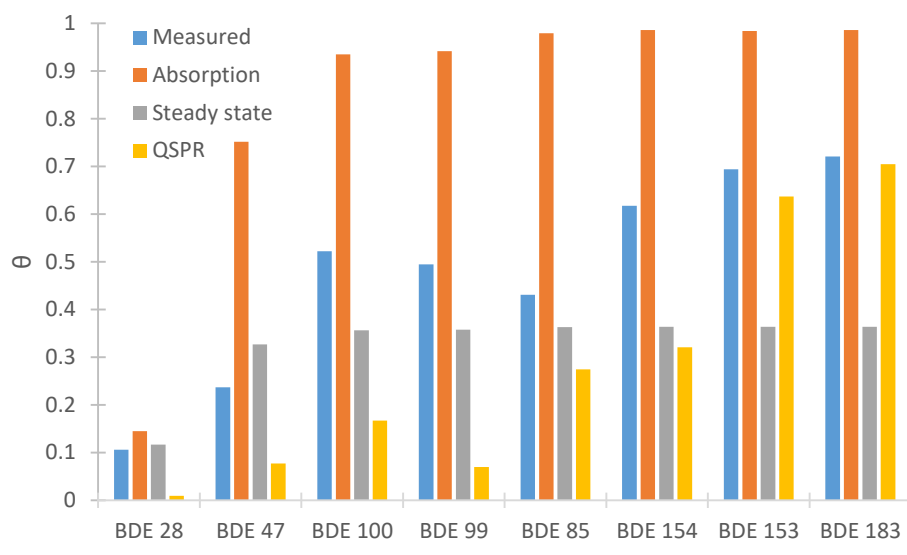


b)

Figure S5: Comparison of measured and predicted θ for all individual PBDEs in summer and winter. Summer was defined as June-August, while winter was defined as December-February



a)



b)

Figure S6: Comparison of the predicted and measured $\log K_p$ (a) and θ (b) using the average conditions at the sampling site (i.e. $T=281.8$ K, $PM_{10}=19.6 \mu\text{g.m}^{-3}$)

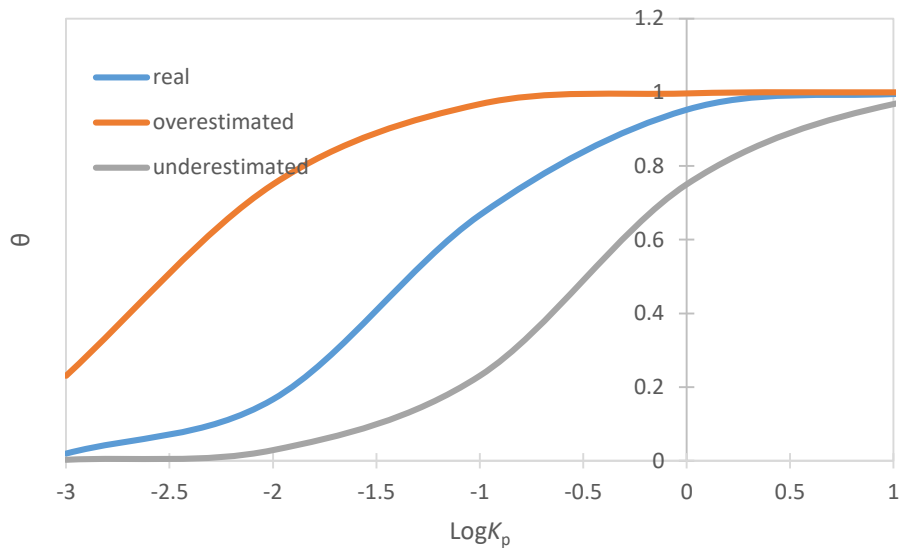


Figure S7: Schematic of the effect of an over- or under-estimation of K_p by one order of magnitude in terms of θ . The average PM_{10} concentrations ($19.6 \mu\text{g.m}^{-3}$) at the sampling site during this study was used.

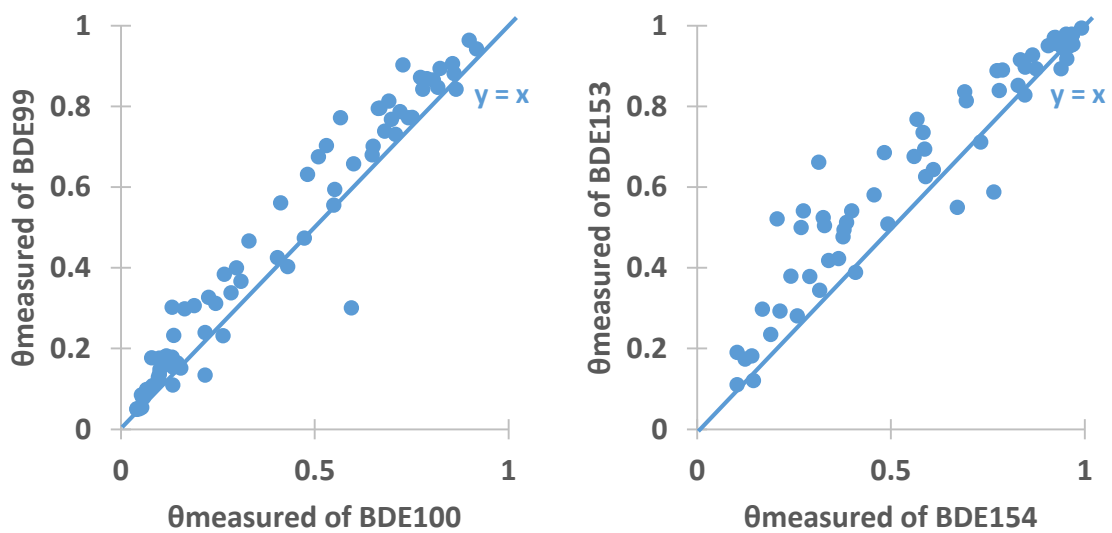
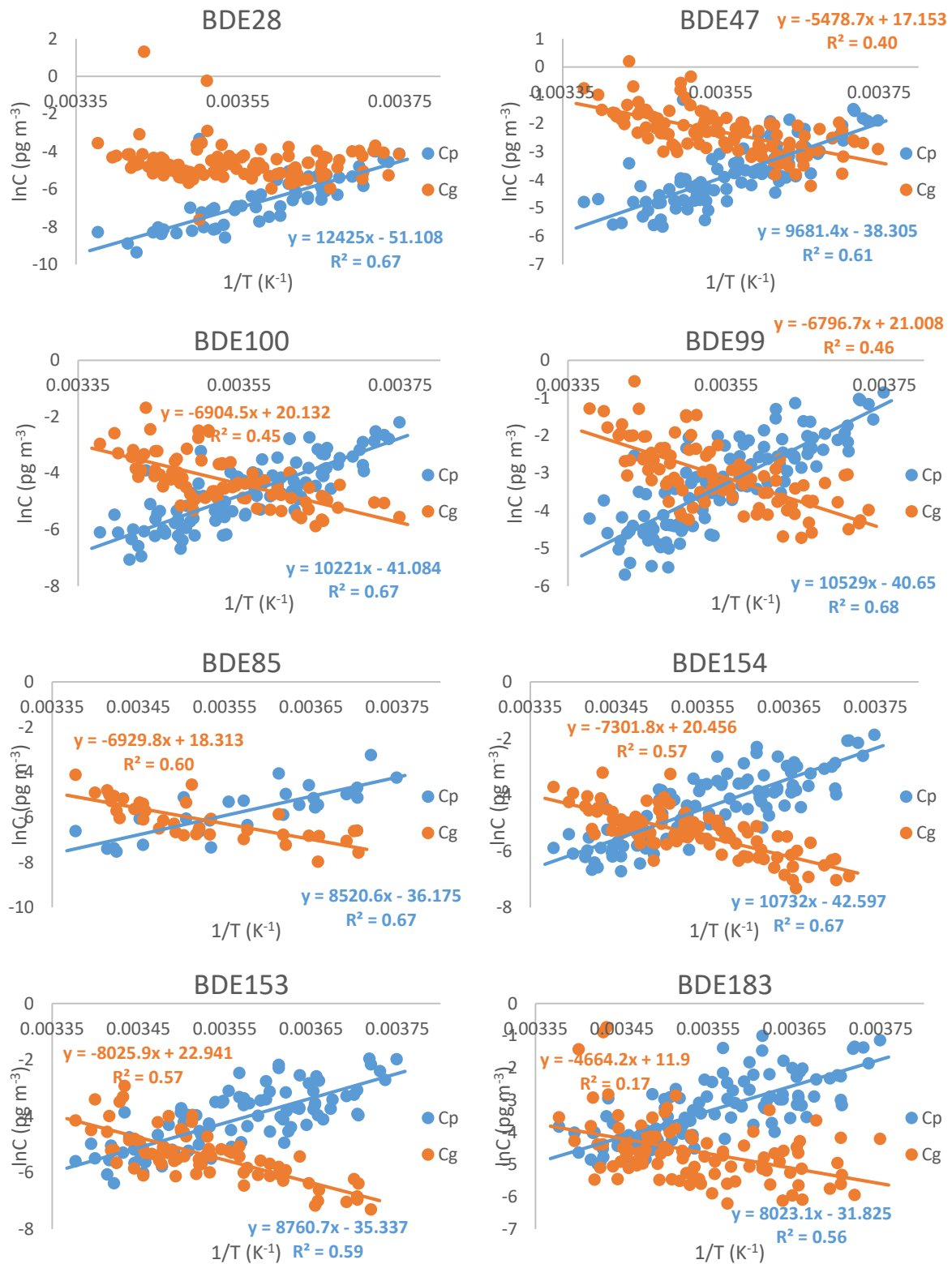


Figure S8: Comparison of the measured particulate fractions (θ_{measured}) of two sets of isomers. Cases when each isomers were detected in both the gaseous and particulate phases were considered



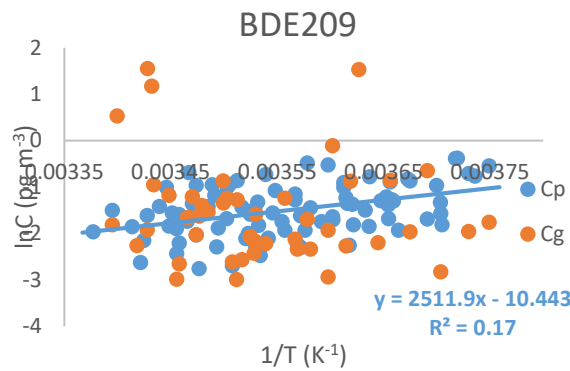


Figure S9: Correlation between the gaseous (orange dots) or the particulate (blue dots) concentration of individual PBDEs (ln transformed) with the inverse of temperature. The regression lines are shown only for cases statistically significant ($p < 0.05$)

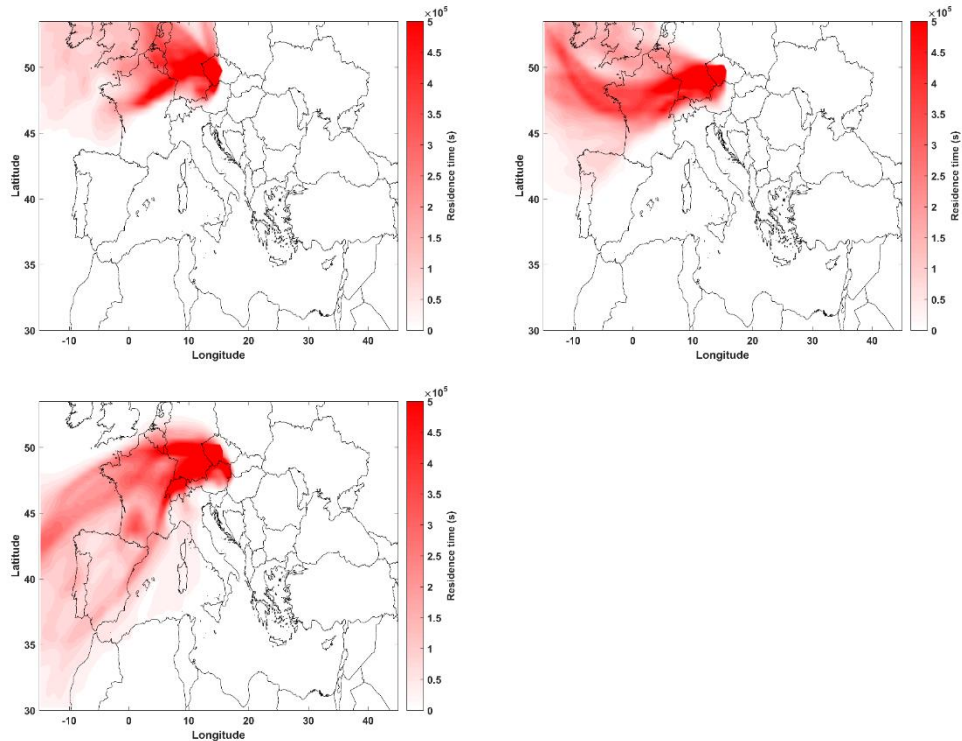


Figure S10: Selected examples of 5 days backward trajectories of samples associated with the lowest PBDE concentrations

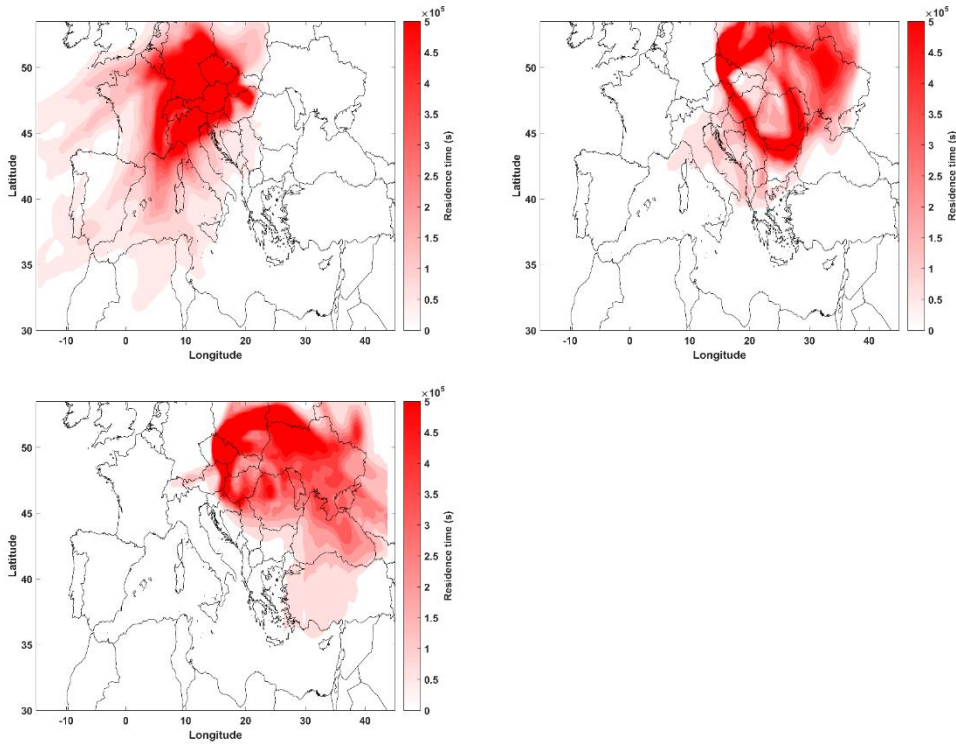


Figure S11: Selected examples of 5 days backward trajectories of samples associated with the highest PBDE concentrations

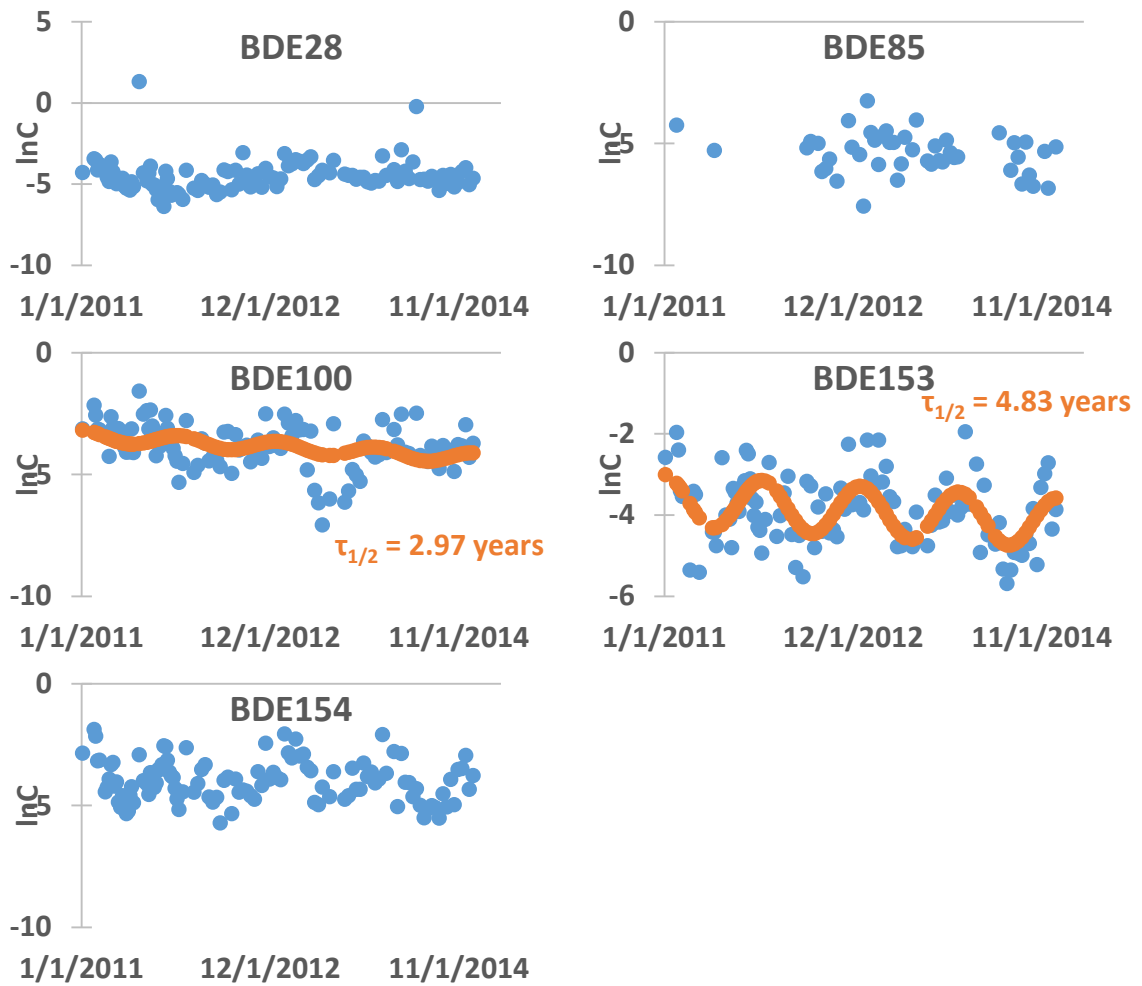


Figure S12: Multi-years trend of some PBDEs